Effects of the ionic size-asymmetry around a charged nanoparticle: unequal charge neutralization and electrostatic screening

Guillermo Iván Guerrero-García,[ab] Enrique González-Tovar†[a] and Mónica Olvera de la Cruz*[b]

Received 20th November 2009, Accepted 7th February 2010
First published as an Advance Article on the web 26th March 2010
DOI: 10.1039/b924438g

We study the consistent inclusion of ionic size-asymmetry for a wide range of macroparticle charges in the primitive model of an electrical double layer around a spherical colloid using (1) Monte-Carlo simulations, (2) the hybrid integral-equation formalism of hypernetted-chain (HNC) and mean-spherical approximation (MSA), and (3) the Gouy–Chapman theory modified for unequal ionic radii. In our simulations, for a weakly charged macroion, we observe surface charge amplification from adsorption of like-charged ions, as well as charge reversal due to overcompensation of the bare nanoparticle charge by counterions. When the nanoparticle charge increases, we detect both asymmetric neutralization and asymmetric electrostatic screening that depend on the sign of the macroion's valence. Specifically, there exists a higher reduction of the original bare charge and a smaller electrostatic potential for the case of negative nanoparticles with positive small counterions, *versus* the case of positive nanoparticles with negative large counterions. These coarse-grained results are in agreement with the predictions of asymmetric charge renormalization (P. González-Mozuelos and M. Olvera de la Cruz, *Phys. Rev. E*, 2009, **79**, 031901), in which the aqueous solvent is explicitly taken into account. Results from the Gouy–Chapman theory modified for unequal ionic radii differ notably from our obtained Monte-Carlo data, while good agreement exists between simulation results and HNC/MSA-treatment findings.

I. Introduction

The study of charged nanoparticles and colloidal solutions is of great relevance due to the enormous potential of technological applications in both industry and biological sciences,[1–4] such as diagnostics[5–7] and photonics.[8–10] Colloidal dispersions can be readily controlled *via* osmotic pressure, salt concentration, as well as pH-variation, in order to generate unique materials[11,12] *via* well defined self-assembly routes.[13–17] These applications rely on effectively controlling the underlying interactions that are mainly repulsive.[18–21] Recent experiments demonstrate clustering near surfaces of charged colloidal systems of negative particles and not of the opposite, positive kind.[22] This observed charge-dependent asymmetry suggests that many important physical quantities should be further analyzed, which will require the development of more robust models that can include specific interactions between ions and the solvent, among other details.

Incidentally, such characteristics of colloidal solutions as the regimes of stability and flocculation and the values of the zeta potential[1,2] are very relevant from a practical viewpoint. For dilute colloidal systems, these properties depend mainly on the ionic structure formed around a single charged macroion—the so-called electrical double layer—that reflects the many-body electrostatic and entropic correlations among the colloids, ions and solvent particles.

Historically, the Gouy–Chapman model[23,24] describes the charge at the colloidal surface as being balanced by a diffuse ionic layer of punctual charged ions. In the Poisson–Boltzmann picture, this representation gives unrealistic values of local ionic concentration close to the colloidal surface. This theoretical failure then motivated the development of the Stern model,[25] in which the total ionic charge is separated into two parts: an adsorbed layer at the locus of the hydrated ions (known as the Stern or Helmholtz plane) and a diffuse layer (or Gouy–Chapman layer) beyond it. Additionally, the Stern model proposed that the ions in the diffuse layer interact with the charged surface only *via* electrostatic interactions, while the ions at the Stern layer can have a chemical affinity for the surface that allows them to be specifically adsorbed *via* covalent bonds or van der Waals forces.

This model was further refined by Grahame[26] in the triple-layer model, wherein a distinction is made between the location of the Stern layer (localized at the inner Helmholtz plane) and the location where the Gouy–Chapman layer begins (outer Helmholtz plane). The ions that are specifically adsorbed at the inner Helmholtz plane are known as specific ions, whereas the point-ions that are in the diffuse layer beyond the outer Helmholtz plane are called indifferent ions due to their electrostatic-only interaction with a charged colloid.

For a binary electrolyte, if only indifferent ions are present in the electrical double layer and one ionic species is allowed to reach the inner Helmholtz plane, the corresponding Poisson–Boltzmann equations reduce to the unequal-radius-modified

[a]*Instituto de Física, Universidad Autónoma de San Luis Potosí, Álvaro Obregón 64, 78000 San Luis Potosí, San Luis Potosí, México*
[b]*Department of Chemistry and Department of Materials Science and Engineering, Northwestern University, Evanston, Illinois 60208, USA*
† Present address: Grupo de Física de Fluidos y Biocoloides, Departamento de Física Aplicada, Universidad de Granada, 18071 Granada, España.

Gouy–Chapman theory, first proposed by Valleau and Torrie for planar geometry.[27] However, the ionic size asymmetry therein is included inconsistently, since the size effects of ions are treated only with respect to the colloid (through the Helmholtz planes), while they see one another still as point ions.

When the ionic size and the size asymmetry are taken into account consistently, counterintuitive phenomena not predicted by the unequal-radius-modified Gouy–Chapman theory occur, such as the local overcompensation of the bare colloidal charge by counterions (charge reversal), at highly charged surfaces, due to ionic size correlations, or the non-dominance of the counterions.[28,29] Additionally, for weakly charged macroions, the inclusion of the ionic size asymmetry predicts attraction of like-charged ions to the first ionic layer on the colloidal surface (surface charge amplification).[30–32] In surface charge amplification, the first layer of adsorbed co-ions amplifies the bare colloidal charge without the additional inclusion of specific interactions. Although this phenomenon is also predicted by the simplistic size-asymmetric Poisson–Boltzmann-like theories,[31,33] the unequal-radius-modified Gouy–Chapman approach differs notably from Monte Carlo simulations in the primitive model.[29]

On the other hand, it is well known that the extent of the electrical double layer determines the microscopic properties of a solution, since it provides information on the interaction range among the colloids. For highly charged like colloids, it is expected that they repel one another due to long-range interactions, which then increases the solubility of the underlying solution. However, if the electrical double layer around each macroparticle is very compact, short range interactions such as van der Waals forces between like charges can become important. This behavior can be understood in terms of charge renormalization as follows: a stronger reduction of the bare charge implies a lower solubility in a dilute colloidal suspension. González-Mozuelos and Olvera de la Cruz[34] have recently demonstrated, theoretically, the existence of asymmetric charge renormalization that explains some of the aforementioned experimental observations;[22] specifically, it has been found that the negative charged nanoparticles are *effectively* less charged than the positive ones of comparable magnitude when a simplified explicit model of the solvent (water) is employed, while slight asymmetries are also reported in small nanoparticles by using the SPC/E explicit solvent water model.[35]

This behavior could also be explained alternatively, or complementarily, at the level of a coarse-grained model, wherein the solvent is a continuous media and different effective hydration-radii for the ionic species are considered. Indeed, the most primitive models of ion solubility, such as the Born solubility model, include the size of these ions as a fundamental parameter. Therefore, the solvent can be taken into account implicitly by using different effective radii for the cations and anions of the salt. In the present work, we precisely explain the physical consequences of this coarse-grained model for the system of an electrical double layer around a spherical macroion by employing (1) Monte-Carlo (MC) simulations, (2) an integral equation-theory based on the hypernetted-chain formalism and mean-spherical approximation (HNC/MSA), and (3) a quasi-point-like Poisson–Boltzmann scheme in the guise of unequal-radius-modified Gouy–Chapman (URMGC) treatment. In particular, we show that both the colloidal-charge neutralization and electrostatic screening of a spherical macroion behave unequally as functions of the colloidal-charge sign, due to the presence of a size-asymmetric electrolyte that is not only in agreement with the findings of González-Mozuelos *et al.*[34] at high colloidal-charges, but also consistent with electro-kinetics experiments near the point of zero charge.[36,37]

This paper is structured as follows. The model system and the theoretical and simulation formalisms employed are detailed in Section II. In Section III, the main results of this work are presented and discussed. Finally, a summary of relevant findings and some concluding remarks are given in Section IV.

II. Theoretical formalism

A. Model system

In this work, we consider an infinitely-diluted colloidal solution that contains a single spherical macroion, of radius and valence r_M and z_M, respectively, which is immersed in a continuum solvent of dielectric constant ε. The colloidal sphere has an associated constant surface-charge density $\sigma_0 = z_M e/4\pi r_M^2$, where e denotes the protonic charge, and is surrounded by a binary electrolyte. In the primitive model, the colloidal macroion and the ions are modeled as hard spheres of radii r_i ($i = M$, +, −) along with embedded punctual charges, $q_i = z_i e$, at their respective centers. For definitiveness, the cations have been chosen as the smallest species of the binary electrolyte; that is, $r_+ < r_-$, with the ratio between the ionic radii $r_-/r_+ = 2$ analogous to what has been used in prior works.[29,38,39] Thus, the interaction potential for a macroion-ion pair and an ion-ion pair is given by

$$U_{ij}(r) = \begin{cases} \infty, & \text{for } r < r_i + r_j, \\ q_i q_j/(4\pi\,\varepsilon_0 \varepsilon\, r), & \text{for } r \geq r_i + r_j, \end{cases} \quad (1)$$

where the subscripts $\{i, j\} = M$, +, − and r denote the distance between the centers of two particles of types i and j. A schematic representation of our model system is shown in Fig. 1.

B. HNC/MSA and URMGC theories

In the past, several theoretical approaches have been used to study the electrical double layer, such as integral equations,[28,40,41] density-functional theories,[42–45] and modified Poisson–Boltzmann schemes.[46] Among these theoretical methodologies, integral equations with the hypernetted-chain closure and mean spherical

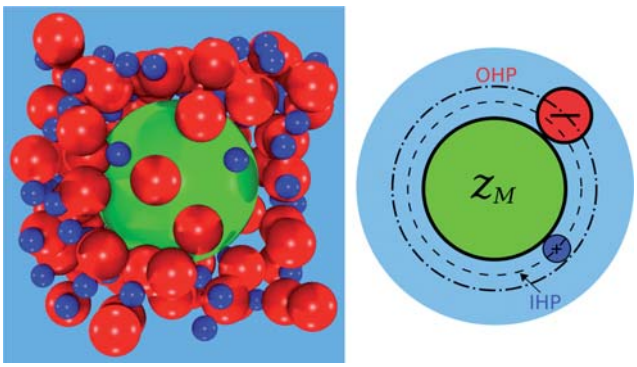

Fig. 1 The model system (snapshot obtained from our MC simulations, on the left) and schematic representation of the inner Helmholtz plane (IHP) and outer Helmholtz plane (OHP) around the macroion.

approximation (HNC/MSA) have shown good agreement with simulation results for Coulombic systems of several geometries,[47–49] including the case of asymmetric ion-sizes.[29] As such, we use here the HNC/MSA-theory.

The Ornstein–Zernike equation for a dispersion of infinitely diluted macroions ($\rho_M = 0$) in the HNC/MSA-approximation that corresponds to our binary-electrolytic system can be written as:[28]

$$h_{Mj}(r) = c_{Mj}(r) + \sum_{k=+,-} \rho_k \int h_{Mk}(t) c_{kj}(|\vec{r} - \vec{t}|)\, dV \quad \text{for } j = +, - \tag{2}$$

where the $c_{Mj}(r) = -\beta U_{Mj}(r) + h_{Mj}(r) - \ln [h_{Mj}(r) + 1]$ corresponds to the HNC closure and the $c_{kj}(|\vec{r} - \vec{t}|)$ takes on the analytical expressions from MSA for bulk electrolytes.[50,51] As presented, eqn (2) comprises a complete set of integral equations for the spherical, electrical double layer that can be solved numerically using an iterative Picard method.[47]

On the other hand, if the HNC closure is used for the $c_{Mj}(r)$ and the expression $c_{kj}(|\vec{r} - \vec{t}|) = -\beta q_k q_j/(\varepsilon|\vec{r} - \vec{t}|)$ is inserted in eqn (2), the integral-equation version of the unequal-radius-modified Gouy–Chapman theory in spherical geometry is obtained. We note that, under this approximation, the ionic-size correlations between electrolyte ions are neglected.

In order to clearly establish the primitive and quasi-punctual models employed in our simulation and theoretical approaches, let us introduce the quantities of macroion-ion contact distances, denoted by d_{M+} and d_{M-}, to be given in the following:

$$d_{Ml} = \begin{cases} (r_M + r_+), & \text{for } l = +, \text{ in MC simulations,} \\ & \text{HNC/MSA and URMGC,} \\ (r_M + r_-), & \text{for } l = -, \text{ in MC simulations,} \\ & \text{HNC/MSA and URMGC} \end{cases} \tag{3}$$

Therefore, in the MC simulations, HNC/MSA and URMGC theories, the asymmetry in size between the ions and the macroion is always taken into account *via* a closest-approach distance that is different for each ionic species. In particular, d_{M+} corresponds to the inner Helmholtz "plane" (IHP), and d_{M-} to the outer Helmholtz "plane" (OHP) as is shown schematically in Fig. 1, and as is discussed in the Introduction (note that in spherical geometry, the Helmholtz planes correspond to concentric shells which become flat surfaces when $r_M \to \infty$).

Analogously, the ion-ion contact distances, $d_{+\,+}$, $d_{-\,-}$, and $d_{+\,-} (= d_{-\,+})$, are respectively given by

$$d_{ij} = \begin{cases} 2r_+, & \text{for } i = j = +, \text{ in MC simulations} \\ & \text{and HNC/MSA,} \\ 2r_-, & \text{for } i = j = -, \text{ in MC simulations} \\ & \text{and HNC/MSA,} \\ (r_+ + r_-), & \text{for } i = + \text{ and } j = -, \text{ in MC} \\ & \text{simulations and HNC/MSA,} \\ 0, & \text{for any value of } i \text{ and } j, \text{ in URMGC} \end{cases} \tag{4}$$

Here, we observe that in the URMGC theory, the ions interact among themselves as point charges while they take on a finite size in both simulations and the integral-equation approach. Thus, these macroion-ion and ion-ion closest-approach distances determine the quasi-point-like nature of these ions associated with the URMGC scheme and show that the excluded-volume effect is taken into account consistently only in MC simulations and in the HNC/MSA-theory.

In addition, very important structural information can be calculated from the radial distribution functions, such as the integrated charge, namely,

$$P(r) = z_M + \sum_{i=+,-} \int_0^r z_i \rho_i g_i(t) 4\pi t^2 dt \tag{5}$$

and the mean electrostatic-potential,

$$\psi(r) = \frac{e}{4\pi\varepsilon_0\varepsilon} \int_r^\infty \frac{P(t)}{t^2} dt \tag{6}$$

The integrated charge is a measure of the net charge (in units of e) inside a sphere of radius r centered at the macroion. At the colloidal surface, we impose $P(r_M) = z_M$, and $P(r \to \infty) = 0$ due to the electroneutrality condition. We note that when $P(r)z_M < 0$, the counterions not only neutralize the native colloidal charge but also somewhat overcompensate it, resulting in a net charge of opposite sign to z_M. Such behavior represents the so-called charge reversal[28–30] (see Fig. 2). It is possible to observe experimentally the phenomenon of charge reversal[52–55] when the integrated charge associated to a sphere of radius r^* corresponds to the effective charge of the macroion and $P(r^*)z_M < 0$.

On the other hand, surface charge amplification can also occur if $P(r)z_M > 0$ and $|P(r)| > |z_M|$, since in this case, the macroion is adsorbing ions of the same sign as its bare charge, z_M, which would increase the original bare charge at the surface. We refer here to this phenomenon as surface charge amplification[31] (see Fig. 2). Though this phenomenon has been misleadingly referred to as "overcharging" in previous works,[30,32,33] we term it here as surface charge amplification to avoid confusions with the phenomena of charge reversal. In the presence of a 1 : 1 size-asymmetric electrolyte, surface charge amplification is expected to have a maximum value at the OHP. This means that even if surface charge amplification is present, it is not necessary

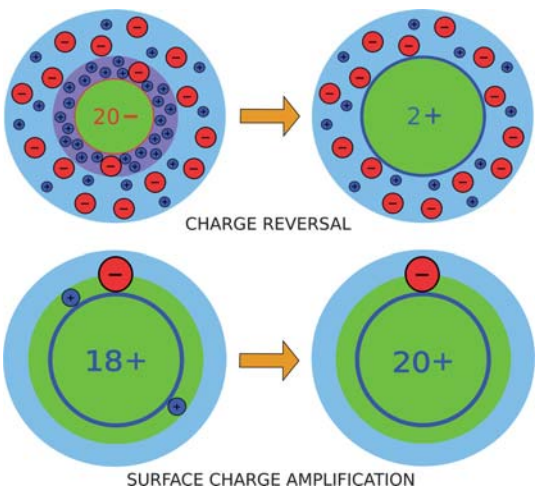

Fig. 2 A schematic representation of charge reversal and surface charge amplification (see explanation in the text).

reflected in the overall effective charge of the colloid away from its surface due to the presence of counterions in the further layers. Thus, the experimental detection of surface charge amplification is more difficult than the detection of charge reversal, since it involves mainly the co-ions being adsorbed between the Helmholtz planes [see inset in Fig. 5(b)]. Moreover, surface charge amplification disappears at high surface charge densities due to the electrostatic repulsion exerted by the macroion over the co-ions. Possible experimental realizations of surface charge amplification could be obtained through the technique used by Cuvillier and Rondelez.[56] Other possibilities to observe surface charge amplification are proposed by Messina.[31]

Regarding the mean electrostatic-potential [eqn (6)], this quantity provides information on the electrostatic screening of the colloidal charge as a function of radial distance from the macroion. In particular, the mean electrostatic-potential in the neighborhood of the Helmholtz zone is usually identified with the zeta potential, ζ, of electrokinetic phenomena (*i.e.*, the potential at the plane of shear or at the slipping plane[1]). Experimentally, the zeta-potential can be measured from phenomena involving a tangential fluid-motion adjacent to a charged surface, as found in electrophoresis, electro-osmosis and streaming current. Thus, a knowledge of the zeta-potential becomes very relevant in physical chemistry because it allows for the characterization of diverse macroscopic features found in charged colloidal systems, which include stability and flocculation properties.[1–4]

Although there exists a conventional and widely accepted definition of the zeta-potential, it is not theoretically possible to exactly predict the localization of the slipping plane. Some experiments suggest that the ζ-potential is located very close to the colloidal surface.[1,57] Moreover, it has been previously shown, theoretically and through simulations, that anomalous curvatures of the mean electrostatic-potential within the restricted primitive model[58] are also present in the case of asymmetric ionic size,[29] which could be relevant in the study of differential capacities in colloidal charged systems.[59–61] For this reason, as well as for the strong relation between the zeta-potential and the mean electrostatic potential near a charged surface, it is very important to analyze the electrostatic potential at the Helmholtz planes. Thus, in the following, we focus on the electrostatic potential at the closest-approach distance of small cations with respect to the macroparticle (or inner Helmholtz plane), identified by ψ_{IHP}, and on the electrostatic-potential associated with the closest-approach distance of large anions with respect to the macroion (or outer Helmholtz plane), denoted by ψ_{OHP} (see Fig. 1).

C. Monte-Carlo simulations

The Monte-Carlo simulations of the spherical electrical double layer consider a cubic box with a macroion fixed at the center under periodic boundary conditions. The electroneutrality of the system is imposed *via* the following relation:

$$N_{-}z_{-} + N_{+}z_{+} + z_{M} = 0 \qquad (7)$$

where N_{-} and z_{-} denote the number and the valence of the anions, respectively; analogously, N_{+} and z_{+} denote the number and the valence of the cations. Lastly, the quantity z_{M} represents the valence of the macroion.

In order to correctly evaluate the long-range Coulombic potential, we use an Ewald-sum approach with conducting boundary-conditions.[62,63] The damping constant α is $5/L$, and the vectors in $\vec{k}$-space, used for calculating the reciprocal-space contribution to the energy, satisfy the condition $k \leq 5$. The length L of the simulation box is determined by the density and the total number of ions, $N_t = N_{-} + N_{+}$, which is between $N_t = 1000$ and $N_t = 2000$. After N_t attempts to move an arbitrary ion, a Monte-Carlo cycle is counted. A thermalization process considers at least 1×10^5 MC cycles, and the canonical average involves from 2×10^5 (for high z_M values) to 1×10^6 (for low z_M values) MC cycles.

III. Results and discussion

In all the calculations reported in this work, we consider a size-asymmetric monovalent binary electrolyte bathing a charged

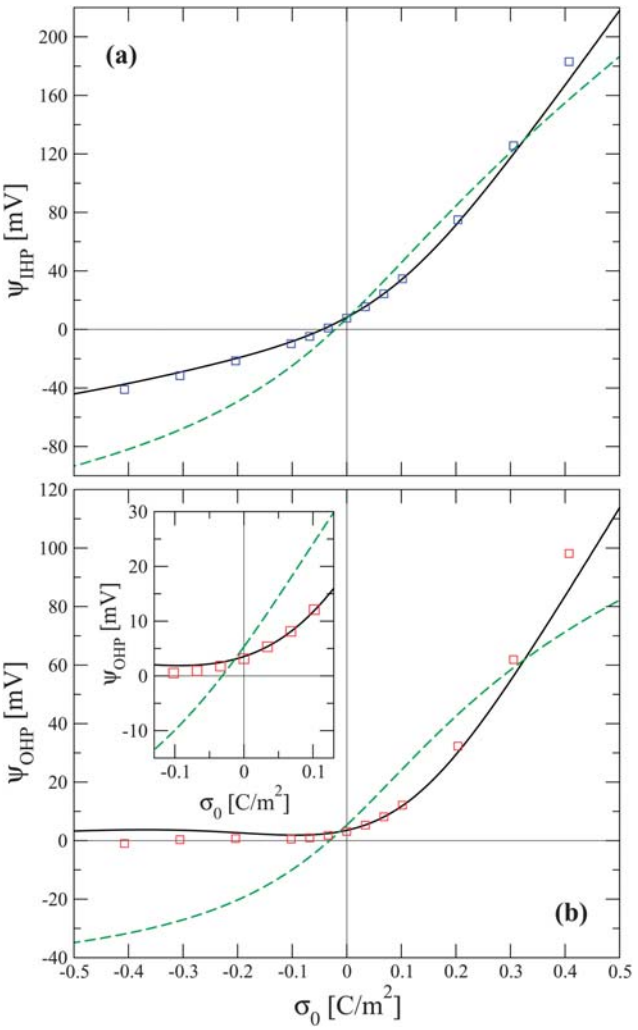

Fig. 3 The mean electrostatic-potential at the Helmholtz planes, as functions of the surface charge density for a 1 : 1, 1 M electrolyte around a macroion of radius $r_M = 15$ Å. The squares, solid lines and dashed lines correspond to an electrolyte of radii $r_{+} = 2.125$ Å and $r_{-} = 4.25$ Å in the MC, HNC/MSA, and URMGC approaches, respectively.

macroparticle of radius $r_M = 15$ Å and of valence z_M, in an aqueous continuum media of dielectric constant and temperature $\varepsilon = 78.5$ and $T = 298$ K, respectively. In the primitive model, the radii of the positive and negative species are $r_+ = 2.125$ Å and $r_- = 4.25$ Å, respectively.

Due to their relevance, in Fig. 3, we plot the mean electrostatic-potential at the inner Helmholtz plane, ψ_{IHP}, and at the outer Helmholtz plane, ψ_{OHP}, as functions of the colloidal surface-charge density, σ_0, obtained *via* MC simulations, and the HNC/MSA and URMGC theories, for a 1 : 1, 1 M size-asymmetric electrolyte around a spherical macroion. In Fig. 3(a), it is observed that, at the point of zero charge ($\sigma_0 = 0$), there exists a non-vanishing electrostatic potential due to the adsorption of small positive cations. This behavior is consistent with the existence of the so-called zero surface-charge double layer originally predicted by Dukhin and coworkers[64,65] more than two decades ago. In fact, this concept has been reviewed recently in an experimental work on the electro-kinetics of uncharged colloids,[37] where the author establishes that "…a double layer might in fact exist, even when there is no electric surface charge at all (on the colloid), solely because of the difference in cation and anion concentrations within the interfacial water layer…" and also provides experimental results supporting this phenomenon. Such difference in cation and anion concentrations (with the corresponding charge separation near the surface of an uncharged colloidal particle) can be ascribed to the difference in the distances of the closest-approach from cations or anions to the colloidal particle, as Dukhin and other authors have proposed.[36,66–70] *On the other hand, far from the point of zero charge*, it is found that the magnitude of ψ_{IHP} is larger for positively charged macroparticles than for negative ones. This would suggest that the small counterions ($z_M < 0$) neutralize and screen the bare colloidal charge more effectively than big counterions ($z_M > 0$). Interestingly, the HNC/MSA results display a good agreement with simulation data, in contrast to the poor concordance of the URMGC results, especially for systems far from the point of zero charge.

In Fig. 3(b), the ψ_{OHP} as a function of σ_0 is illustrated. In this case, the MC simulations and HNC/MSA results show that the ψ_{OHP} is not only smaller in magnitude for the negative values of the macroion's charge, with respect to the positive ones, but also that it can have a positive sign in the region around the point of zero charge [even for negative values of σ_0, see inset of Fig. 3(b)]. This behavior resembles what is observed in the α-alumina zeta-potential measurements by Johnson *et al.*,[36] in the presence of 1 M $LiNO_3$, for varying pH [see Fig. 2(b) of ref. 36]. In that work, it is proved that the zeta-potential is positive in a wide region of pH. Assuming that there is a sign change in the bare colloidal charge within that pH region—as occurs with other monovalent electrolytes in the same work— the Smoluchowski approximation that relates the electrophoretic mobility to the zeta-potential through $\mu = \varepsilon\zeta/\eta$, where η denotes the viscosity, suggests that such positive values in zeta-potential, even for negative charges, are due to a preferential adsorption of the positive (Li^+) ions, which could be explained partially if the ionic-size asymmetry is taken into account in a consistent manner, as has been done here.

To further elucidate how the aforementioned potential-charge behavior arises naturally from our model, let us first consider an uncharged colloidal particle of radius $r_M = 15$ Å surrounded by a 1 : 1, 1 M size-asymmetric binary electrolyte of radii $r_+ = 2.125$ Å and $r_- = 4.25$ Å. The corresponding profiles of radial distribution functions, $g_{Mj}(r)$, integrated charge $P(r)$, and mean electrostatic-potential $\psi(r)$, are plotted in Fig. 4 [$g_{Mj}(r)$ in the main panel, and $P(r)$ and $\psi(r)$ in the insets]. In this figure, we observe from the $g_{Mj}(r)$ of MC and HNC/MSA that the small cations are adsorbed in a region between the Helmholtz planes that is inaccessible to the anions. This asymmetric behavior results in a mean electrostatic-potential taking on a value different from zero at the IHP, as well as in the adsorption of finite charge at the OHP in the case of a charge-neutral colloidal particle.

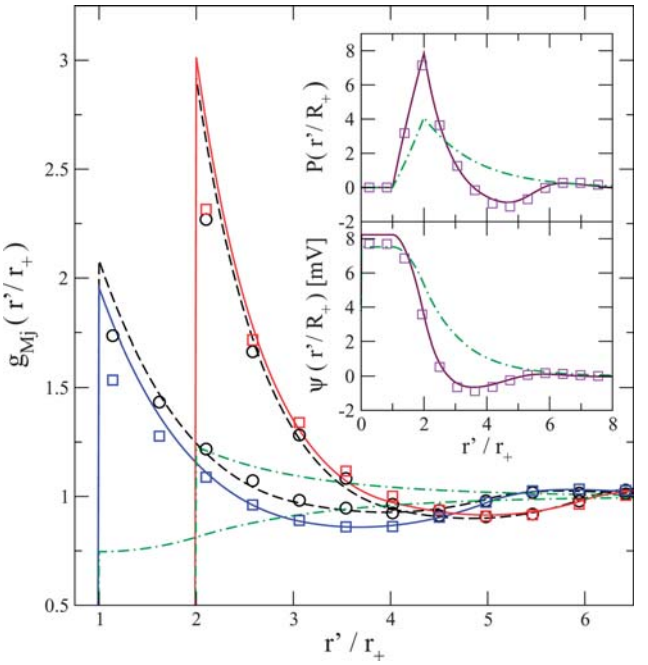

Fig. 4 Radial distribution functions, $g_{Mj}(r)$, integrated charge, $P(r)$, and mean electrostatic-potential, $\psi(r)$, as functions of the distance to a spherical uncharged colloid of radius 15 Å. The squares, solid lines and dot-dashed lines correspond to the MC, HNC/MSA and URMGC results, respectively, associated to a 1 : 1, 1 M, size-asymmetric electrolyte of radii $r_+ = 2.125$ Å and $r_- = 4.25$ Å. The circles and dashed lines (main panel) correspond to the $g_{Mj}(r)$ of a 1 M hard spheres mixture of radii $r_1 = 2.125$ Å and $r_2 = 4.25$ Å, obtained *via* MC simulations and HNC/MSA calculations. Here and in the rest of the figures, the distance r' is measured from the colloid surface.

In order to explain the origin of this adsorption, we now consider two limiting cases: (i) when the electrolyte has a non-zero size while interacting with the uncharged colloid but is considered punctual when interacting with other ions (URMGC theory) and (ii) when the electrolyte is uncharged (that is, in the limit when it is simply a size-asymmetric hard sphere mixture; see main panel of Fig. 4). When the ionic-size asymmetry is partially taken into account [case (i)], the degree of adsorption of cations and anions occur asymmetrically near the Helmholtz planes, resulting in a non-vanishing mean electrostatic-potential at the IHP as well as a non-zero colloidal net charge being adsorbed (see insets) at the OHP at the zero-charge point. However, these URMGC quantities decay monotonically as functions of the distance beyond the OHP.

In contrast, the radial distribution functions corresponding to the size-asymmetric electrolyte in the primitive model and the size-asymmetric hard-spheres mixture [case (ii)] are very similar. This means that the main contribution to the electrolytic adsorption comes from the hard-sphere depletion forces. These depletion forces are responsible for the incremental intensity-difference in ionic adsorption already seen in the URMGC-theory and as well for the oscillations in the radial distribution functions, integrated charge, and mean electrostatic-potential away from the OHP, as observed in the MC simulations and HNC/MSA results.

Additionally, we note that the adsorption of anions is slightly higher at the OHP when compared with the hard-sphere case, whereas the opposite happens for the cations at the IHP. This behavior can be rationalized when we realize that at the OHP, in addition to the depletion forces attracting the anions towards the uncharged colloidal particle, there are two net competing electrostatic forces: one pushing the aforementioned anions towards the macroparticle, due to the adsorbed small cations in-between the Helmholtz planes, as well as another net electrostatic force pulling the ions away from the colloidal particle, as exerted by the electrolyte in bulk. In this case, the electrostatic attraction due to the layer of adsorbed cations overcomes the electrostatic bulk attraction, and consequently, the adsorption of anions increases with respect to the hard-sphere case. A similar argument can be given for the decrease of the cations near the IHP. We note that, however, when the valence of the ions is increased, the electrostatic bulk attraction over the cations and anions at the point of zero charge can be notably augmented, then resulting in a "drying" of both species at the Helmholtz planes (see *e.g.*, refs 32 and 71).

Let us now consider the same system of electrolyte, but with a charged colloidal particle. In Fig. 5, the radial distribution functions, integrated charges, and mean electrostatic-potentials are presented for $z_M = -12$ [Fig. 5(a)] and $z_M = 12$ [Fig. 5(b)], based on results from MC simulations and the HNC/MSA and URMGC theories. Here, it is seen that for $z_M = -12$, the adsorption of the cations increases at the IHP, while that of the anions decreases at the OHP, when compared to the uncharged case displayed in Fig. 4, given that, for $z_M < 0$, the cations are the counterions and the anions are the co-ions in relation to the macroparticle. We note that the agreement in the mean electrostatic-potential between the URMGC and MC data at the Helmholtz planes deteriorates when compared with the case of the uncharged colloidal particle, while HNC/MSA data display an overall good agreement and exhibit charge reversal (or the overcompensation of the bare colloidal charge by counterions), with a maximum at the OHP, as seen in the inset of the integrated charge in Fig. 5(a). On the other hand, for $z_M = 12$, the opposite behavior in the adsorption of cations (co-ions) and anions (counterions) is observed, as expected. In addition, we note that the magnitude of $\psi(r)$ in the insets of Fig. 5 is higher for URMGC than for MC and HNC/MSA, which would suggest that URMGC could be used as a bound of the electrostatic potential in the primitive model. Nevertheless, although the magnitude of the electrostatic potential at the Helmholtz planes is higher for URMGC than for MC ($|\psi_{URMGC}| > |\psi_{MC}|$) and HNC/MSA ($|\psi_{URMGC}| > |\psi_{HNC/MSA}|$) at highly negative charge values of the macroion, and up to $z_M = 54$ (0.3 C m^{-2} approximately, see Fig. 3), this situation is reversed for highly positively-charged colloidal particles, where surprisingly, the electrostatic screening of point-ions is higher than the MC ($|\psi_{URMGC}| < |\psi_{MC}|$) and HNC/MSA ($|\psi_{URMGC}| < |\psi_{HNC/MSA}|$) results at the Helmholtz planes.

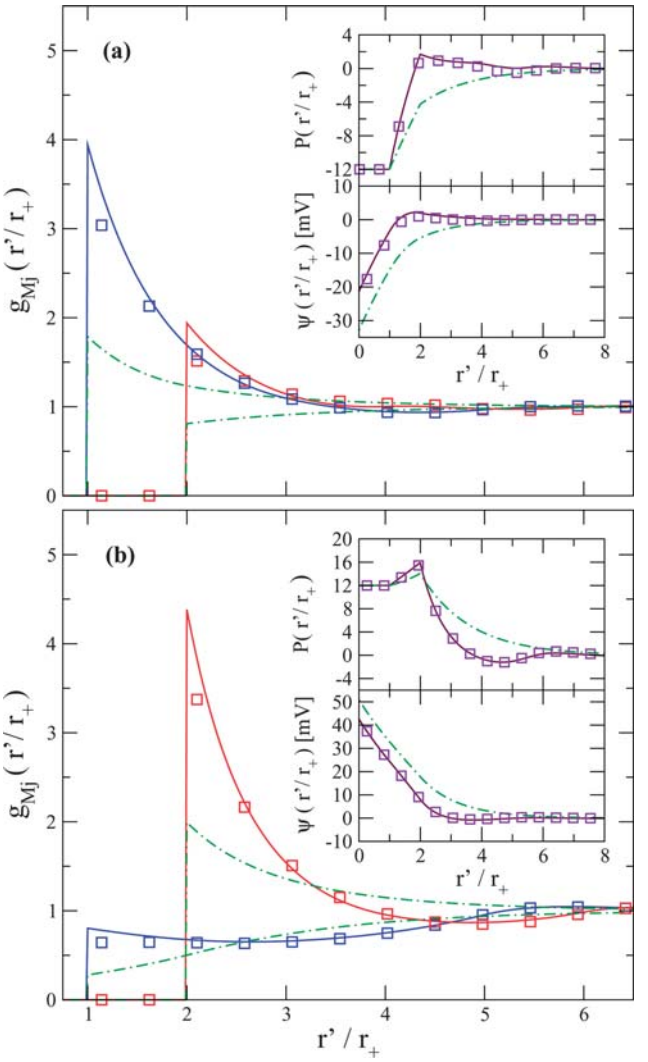

Fig. 5 The radial distribution functions, integrated charge, and mean electrostatic-potential as functions of the distance to a spherical, charged colloid of radius 15 Å. The squares, solid lines and dot-dashed lines are associated to a 1 : 1, 1 M, size-asymmetric electrolyte of radii $r_+ = 2.125$ Å and $r_- = 4.25$ Å for MC, HNC/MSA and URMGC, respectively. In panel (a) the valence of the macroion is $z_M = -12$, whereas in panel (b) $z_M = 12$.

Another interesting observation regarding the integrated-charge profiles for $z_M = 12$ is that co-ions can amplify the magnitude of the native colloidal charge with a maximum surface charge amplification occurring at the OHP, as observed in the inset of Fig. 5(b). Also visible in this graph, is that although URMGC can display maximum surface charge amplification at the OHP, as seen in the corresponding $P(r)$-profile, it also presents an incorrect monotonic behavior away from the OHP that is in contrast with the good agreement found for the integral-equation and MC results.

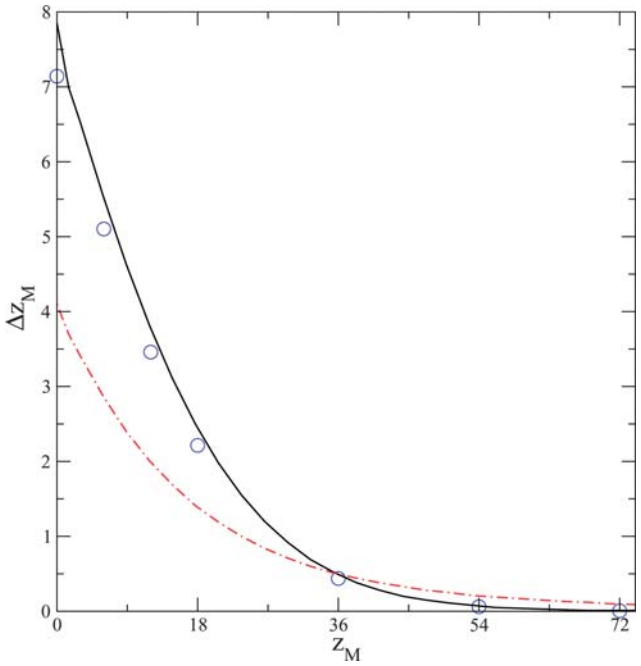

Fig. 6 Adsorbed charge amplification as a function of z_M for a charged macroion of radius $r_M = 15$ Å in the presence of a 1 : 1, 1 M size-asymmetric electrolyte of radii $r_+ = 2.125$ Å and $r_- = 4.25$ Å. The circles, solid line, and dot-dashed line correspond to MC, HNC/MSA, and URMGC results, respectively.

Previously, simulation evidences of surface charge amplification in the size-asymmetric, spherical electrical double layer have been reported for a smaller macroion-size at similar conditions.[32] Therein, it is mentioned that the surface charge amplification decreases when the macroion's charge gets augmented, due to the increase of the electrostatic repulsion over the small co-ions. Here, we quantify this decrease, as well as the accuracy of the theories when compared with MC simulations. As such, let us define the quantity of *adsorbed charge amplification* as the difference between the maximum adsorbed $P(r)$ minus the bare colloidal charge: $\Delta z_M = P(r)_{max} - z_M$. Thus, in Fig. 6, the adsorbed charge amplification corresponding to the case of monovalent ions is plotted as a function of the colloidal charge. In this figure, the MC data show a monotonic decay with respect to the macroion valence, which is well described by HNC/MSA; on the other hand, URMGC only agrees qualitatively.

In order to analyze the colloidal-charge neutralization and screening for highly positive- and negative-macroion charges of the same magnitudes, let us first consider the case in which the ionic-size asymmetry is only partially taken into account, as in URMGC. In Fig. 7, the profiles of integrated charge and of mean electrostatic-potential are plotted as functions of the radial distance for a 1 : 1, 1 M size-asymmetric electrolyte with closest-approach distances $r_+ = 2.125$ Å and $r_- = 4.25$ Å, around a macroion of radius and valence $r_M = 15$ Å and $|z_M| = 36$, 54 and 72, respectively. We observe that the URMGC profiles of integrated charge and the mean electrostatic-potential are monotonic in all cases and that the negative macroion charges

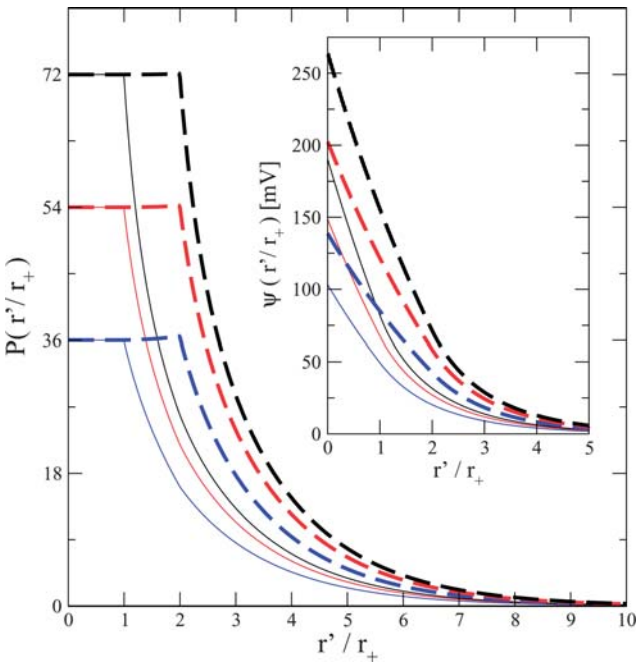

Fig. 7 Integrated charge and mean electrostatic-potential as functions of the distance for a charged macroion of radius $r_M = 15$ Å in presence of a 1 : 1, 1 M, size-asymmetric electrolyte with maximum approach distances $r_+ = 2.125$ Å and $r_- = 4.25$ Å, around a macroion of valence z_M in the URMGC theory. The solid lines correspond to $-P(r)$ (in the main panel) and $-\psi(r)$ (in the inset) for $z_M = -36$, -54, and -72. The dashed lines correspond to $P(r)$ (in the main panel) and $\psi(r)$ (in the inset) for $z_M = 36$, 54, and 72.

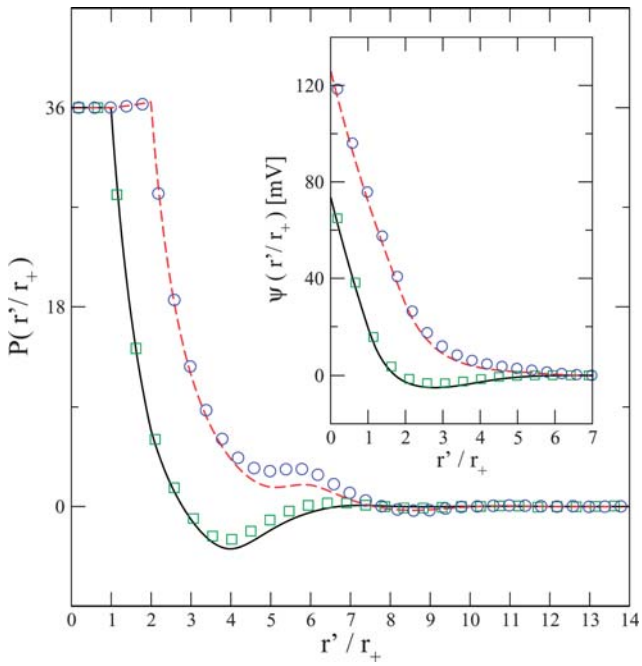

Fig. 8 The integrated charge and mean electrostatic-potential as functions of the distance for a charged macroion of radius $r_M = 15$ Å in the presence of a 1 : 1, 1 M, size-asymmetric electrolyte of radii $r_+ = 2.125$ Å and $r_- = 4.25$ Å. The squares and solid lines correspond to MC and HNC/MSA results, respectively, of $-P(r)$ (in the main panel) and $-\psi(r)$ (in the inset), for $z_M = -36$. The circles and dashed lines correspond to MC and HNC/MSA data, respectively, associated to $P(r)$ (in the main panel) and $\psi(r)$ (in the inset), for $z_M = 36$.

(small counterions) have lower magnitudes of $P(r)$ and $\psi(r)$ when compared with the positive macroion charges (compare solid and dashed lines).

On the other hand, we expect that the ionic-size asymmetry, when taken into account consistently, enhances the behavior already displayed by URMGC, as it can be corroborated in Fig. 8 from the profiles of $P(r)$ and $\psi(r)$ for a 1 : 1, 1 M size-asymmetric electrolyte of radii $r_+ = 2.125$ Å, and $r_- = 4.25$ Å, around a macroion of radius and valence $r_M = 15$ Å and $|z_M| = 36$, respectively. In the integrated-charge profiles (main panel), we observe that the small counterions more efficiently neutralize the colloidal charge, even exhibiting charge reversal. Consistently, in the inset of Fig. 8, it is seen that the mean electrostatic-potential is lower in magnitude for small counterions than for big counterions, not only at the Helmholtz planes (as shown in Fig. 3) but for all values of r plotted. We would like to mention that the last results are in agreement with theoretical and simulation observations of a preferential adsorption of counterions, in size-asymmetric, monovalent electrolytes around a charged cylinder (see Fig. 1 of ref. 72).

IV. Concluding remarks

In this work, we have studied the charge neutralization and electrostatic screening for a size-asymmetric binary electrolyte around a spherical colloid, with special emphasis on the comparison regarding the unequal behaviors for positively and negatively charged colloids. Firstly, at the point of zero charge, it is shown that, in the primitive model, the adsorption process of the size-asymmetric, monovalent electrolytes is mainly due to depletion forces. This mechanism induces a preferential adsorption of the smallest species (irrespective of its sign) to a neutral colloid without the necessity of including additional specific interactions with the colloidal surface if the ionic size-asymmetry and the electrolyte concentration are significant. Complementarily, when the colloidal charge departs from zero, phenomena, such as charge reversal and surface charge amplification occur as consequences of the consistent inclusion of the ionic-size asymmetry in our simulations and theoretical HNC/MSA-integral equation description. In particular, it has been evident that, due to the electrostatic repulsion between the small co-ions and the electrified macroparticle, the surface charge amplification decreases when the colloidal bare charge is increased. This means that, if the co-ions are smaller than the counterions, surface charge amplification is expected to occur at very low colloidal charges and high electrolyte concentrations, as has been shown in this study and in another recent simulation work.[73] The experimental observation of surface charge amplification and the above tendencies could be realized through the technique used by Cuvillier and Rondelez,[56] although other possibilities have been proposed by Messina.[31]

Regarding the results of electro-kinetic experiments in the vicinity of the zero-charge point,[36,37] we mention that although other complex mechanisms could indeed be present, our coarse-grained, ionic-size-asymmetric model has the ability to properly capture notable phenomenology, such as the local adsorption of net charge next to the neutral colloidal surface, as well as the existence of a non-zero mean electrostatic-potential for an uncharged macroparticle. As such, the model used here could act as a starting point, capable of further improvement by the addition of short-range interactions and/or more sophisticated chemical mechanisms.[74]

As a main result of the present study, it is observed that for large σ_0 values, higher charge neutralization and electrostatic screening are associated with negative colloidal charges (*i.e.*, for small counterions) *versus* positive colloidal charges (*i.e.*, for big counterions). This trend is reflected in the behavior of the mean electrostatic-potential profiles at the Helmholtz planes as functions of σ_0. The unequal (or asymmetric) charge neutralization and electrostatic screening observed here are similar to those predicted by González-Mozuelos and Olvera de la Cruz,[34] who found that these phenomena result from the asymmetric adsorption of water over the colloidal surface. In our coarse-grained model, this solvent effect is embodied implicitly by using different effective hydration-radii for the ions. The correspondence between the unequal behavior of negatively and positively charged colloids detected in both approaches is remarkable, considering that our coarse-grained model does not take into account the electrostatic contributions due to the water molecules' ordering around ions and colloid, which could be assumed at first to be more important (for low electrolyte concentrations) than the ionic hydration effects coming from excluded volume. However, for those conditions in which ionic size correlations could be presumed to be dominant, it is expected that the consistent inclusion of ionic size asymmetry (through the use of different effective hydrated ionic radii) could provide a simpler and more economical qualitative description of the electrical double layer, in agreement with (and complementing) the more sophisticated and resource-expensive explicit solvent models.

It is also worthwhile to mention that the ionic hydration has been taken into account in our model in an effective way, such that there is no restriction on the selection of small and big ions for the ionic species. In particular, we have proposed here small cations and big anions based on the experimental observations of electrophoresis mobilities near the point of zero charge, as cited in ref. 36. In addition, we note that the above theoretical predictions are not restricted to very small nanoparticles or very high surface charge densities, and a similar behavior is indeed expected in cylindrical or planar geometries under similar conditions. Thus, the above unequal charge neutralization and electrostatic screening could also be verified experimentally by using well-established protocols[55,75,76] to determine electrophoresis mobilities of a charged colloidal macroparticle in the presence of a size-asymmetric salt at high electrolyte concentrations. On the other hand, an analogous, strong, asymmetric behavior with respect to the surface potential of silica particles in a two-dimensional experimental system has been reported recently.[22] Although the spatial lengths involved in that work and those in our model are different, we believe that our results can be useful in shedding light on the intriguing mechanism behind the attractive interactions observed experimentally among negatively charged colloidal particles that is absent for positive ones.

Finally, in order to apply our coarse-grained model to make more realistic theoretical predictions for these colloidal dispersions, it is necessary to have estimations of the values of effective hydrated radii, which could be obtained from the more detailed and sophisticated molecular models that take solvent,[77–83] as well as image-charge contributions[84,85] explicitly into account.

Acknowledgements

This work was supported by Consejo Nacional de Ciencia y Tecnología (CONACYT, México), through grant CB-2006-01/58470, PROMEP, and by National Science Foundation grant DMR-0520513 of the MRSEC program at Northwestern University. E. G.-T. thanks Centro Nacional de Supercómputo of Instituto Potosino de Investigación Científica y Tecnológica for the computing time in the Cray XD1 and IBM E-1350 machines, and for the computational help by J. Limón, J. Rentería, and J. C. Sánchez at the Centro de Cómputo of Instituto de Física UASLP. G. I. G.-G. acknowledges a post-doctoral fellowship from CONACYT.

References

1 R. J. Hunter, *Zeta Potential in Colloid Science*, Academic Press, New York, 1981.
2 R. J. Hunter, *Foundations of Colloid Science*, Clarendon, Oxford, 1987.
3 F. Fenell-Evans and H. Wennerström, *The Colloidal Domain: Where Physics, Chemistry, Biology and Technology Meet*, Wiley-VCH, New York, 1994.
4 P. C. Hiemenz and R. Rajagopalan, *Principles of Colloid and Surface Chemistry*, Marcel Dekker, New York, 1997.
5 S. J. Park, T. A. Taton and C. A. Mirkin, *Science*, 2002, **295**, 1503; N. L. Rosi and C. A. Mirkin, *Chem. Rev.*, 2005, **105**, 1547.
6 S. Y. Park, A. K. R. Lytton-Jean, B. Lee, S. Weigand, G. C. Schatz and C. A. Mirkin, *Nature*, 2008, **451**, 553; D. Nykypanchuk, M. M. Maye, D. van der Lelie and O. Gang, *Nature*, 2008, **451**, 549.
7 R. Dreyfus, M. E. Leunissen, R. J. Sha, A. V. Tkachenko, N. C. Seeman, D. J. Pine and P. M. Chaikin, *Phys. Rev. Lett.*, 2009, **102**, 048301.
8 P. V. Braun and P. Wiltzius, *Nature*, 1999, **402**, 603.
9 A. M. Kalsin, M. Fialkowski, M. Paszewski, S. K. Smoukov, K. J. M. Bishop and B. A. Grzybowski, *Science*, 2006, **312**, 420.
10 M. C. George, A. Mohraz, M. Piech, N. S. Bell, J. A. Lewis and P. V. Braun, *Adv. Mater.*, 2009, **21**, 66.
11 M. Leunissen, J. Zwanikken, R. van Roij, P. M. Chaikin and A. van Blaaderen, *Phys. Chem. Chem. Phys.*, 2007, **9**, 6405; M. Leunissen, A. van Blaaderen, A. D. Hollingsworth, M. T. Sullivan and P. M. Chaikin, *Proc. Natl. Acad. Sci. U. S. A.*, 2007, **104**, 2585.
12 D. Lee, Z. Gemici, M. F. Rubner and R. E. Cohen, *Langmuir*, 2007, **23**, 8833.
13 I. Szleifer, O. V. Gerasimov and D. H. Thompson, *Proc. Natl. Acad. Sci. U. S. A.*, 1998, **95**, 1032.
14 S. Graves, K. Meleson, J. Wilking, M. Y. Lin and T. G. Mason, *J. Chem. Phys.*, 2005, **122**, 134703.
15 G. R. Maskaly, R. E. Garcia, W. C. Carter and Y. M. Chiang, *Phys. Rev. E: Stat., Nonlinear, Soft Matter Phys.*, 2006, **73**, 011402.
16 P. J. Lu, E. Zaccarelli, F. Ciulla, A. B. Schofield, F. Sciortino and D. A. Weitz, *Nature*, 2008, **453**, 499.
17 B. A. Grzybowski, C. E. Wilmer, J. Kim, K. P. Browne and K. J. M. Bishop, *Soft Matter*, 2009, **5**, 1110.
18 T. M. Squires and M. P. Brenner, *Phys. Rev. Lett.*, 2000, **85**, 4976.
19 S. H. Behrens and D. G. Grier, *Phys. Rev. E: Stat., Nonlinear, Soft Matter Phys.*, 2001, **64**, 050401.
20 Y. Levin, *Rep. Prog. Phys.*, 2002, **65**, 1577.
21 H. Boroudjerdi, Y. W. Kim, A. Naji, R. R. Netz, X. Schlagberger and A. Serr, *Phys. Rep.*, 2005, **416**, 129.
22 E. W. Gomez, N. G. Clack, H. J. Wu and J. T. Groves, *Soft Matter*, 2009, **5**, 1931.
23 M. Gouy, *J. Phys. Theor. Appl.*, 1910, **9**, 457.
24 D. L. Chapman, *Philos. Mag.*, 1913, **25**, 475.
25 O. Stern, *Z. Elektrochem.*, 1924, **30**, 508.
26 D. C. Grahame, *Chem. Rev.*, 1947, **41**, 441.
27 P. Valleau and G. M. Torrie, *J. Chem. Phys.*, 1982, **76**, 4623.
28 G. I. Guerrero-García, E. González-Tovar, M. Lozada-Cassou and F. de J. Guevara-Rodríguez, *J. Chem. Phys.*, 2005, **123**, 034703.
29 G. I. Guerrero-García, E. González-Tovar and M. Chávez-Páez, *Phys. Rev. E: Stat., Nonlinear, Soft Matter Phys.*, 2009, **80**, 021501.
30 F. Jiménez-Ángeles and M. Lozada-Cassou, *J. Phys. Chem. B*, 2004, **108**, 7286.
31 R. Messina, *J. Chem. Phys.*, 2007, **127**, 214901.
32 G. I. Guerrero-García, E. González-Tovar, M. Chávez-Páez and M. Lozada-Cassou, *J. Chem. Phys.*, 2010, **132**, 054903.
33 J. Yu, G. E. Aguilar-Pineda, A. Antillón, S.-H. Dong and M. Lozada-Cassou, *J. Colloid Interface Sci.*, 2006, **295**, 124.
34 P. González-Mozuelos and M. Olvera de la Cruz, *Phys. Rev. E: Stat., Nonlinear, Soft Matter Phys.*, 2009, **79**, 031901.
35 W. Kung, P. González-Mozuelos and M. Olvera de la Cruz, *Soft Matter*, 2010, **6**, 331.
36 S. B. Johnson, P. J. Scales and T. W. Healy, *Langmuir*, 1999, **15**, 2836.
37 A. Dukhin, S. Dukhin and P. Goetz, *Langmuir*, 2005, **21**, 9990.
38 H. Greberg and R. Kjellander, *J. Chem. Phys.*, 1998, **108**, 2940.
39 T. Terao and T. Nakayama, *Phys. Rev. E: Stat., Nonlinear, Soft Matter Phys.*, 2001, **63**, 041401.
40 E. González-Tovar and M. Lozada-Cassou, *J. Phys. Chem.*, 1989, **93**, 3761.
41 F. Jiménez-Ángeles and M. Lozada-Cassou, *J. Chem. Phys.*, 2008, **128**, 174701.
42 T. Goel and C. N. Patra, *J. Chem. Phys.*, 2007, **127**, 034502.
43 T. Goel, C. N. Patra, S. K. Ghosh and T. Mukherjee, *J. Chem. Phys.*, 2008, **129**, 154906.
44 T. Goel, C. N. Patra, S. K. Ghosh and T. Mukherjee, *Mol. Phys.*, 2009, **107**, 19.
45 C. N. Patra, *J. Phys. Chem. B*, 2009, **113**, 13980.
46 S. Lamperski, C. W. Outhwaite and L. B. Bhuiyan, *J. Phys. Chem. B*, 2009, **113**, 8925.
47 S. Lozada-Cassou, R. Saavedra-Barrera and D. Henderson, *J. Chem. Phys.*, 1982, **77**, 5150.
48 M. Deserno, F. Jiménez-Ángeles, C. Holm and M. Lozada-Cassou, *J. Phys. Chem. B*, 2001, **105**, 10983.
49 R. Messina, E. González-Tovar, M. Lozada-Cassou and C. Holm, *Europhys. Lett.*, 2002, **60**, 383.
50 L. Blum, *Mol. Phys.*, 1975, **30**, 1529.
51 K. Hiroike, *Mol. Phys.*, 1977, **33**, 1195.
52 K. Besteman, M. A. G. Zevenbergen, H. A. Heering and S. G. Lemay, *Phys.Rev. Lett.*, 2004, **93**, 170802.
53 K. Besteman, M. A. G. Zevenbergen and S. G. Lemay, *Phys. Rev. E: Stat., Nonlinear, Soft Matter Phys.*, 2005, **72**, 061501.
54 F. H. J. van der Heyden, D. Stein, K. Besteman, S. G. Lemay and C. Dekker, *Phys. Rev. Lett.*, 2006, **96**, 224502.
55 A. Martín-Molina, C. Rodríguez-Beas, R. Hidalgo-Álvarez and M. Quesada-Pérez, *J. Phys. Chem. B*, 2009, **113**, 6834.
56 N. Cuvillier and F. Rondelez, *Thin Solid Films*, 1998, **327**, 19.
57 J. Israelachvili and G. Adams, *J. Chem. Soc., Faraday Trans. 1*, 1978, **74**, 975.
58 E. González-Tovar, F. Jiménez-Ángeles, R. Messina and M. Lozada-Cassou, *J. Chem. Phys.*, 2004, **120**, 9782.
59 M. B. Partenskii and P. C. Jordan, *Condens. Matter Phys.*, 2005, **8**, 397.
60 M. B. Partenskii and P. C. Jordan, *Phys. Rev. E: Stat., Nonlinear, Soft Matter Phys.*, 2008, **77**, 061117.
61 M. B. Partenskii and P. C. Jordan, *Phys. Rev. E: Stat., Nonlinear, Soft Matter Phys.*, 2009, **80**, 011112.
62 M. P. Allen and D. J. Tildesley, *Computer Simulation of Liquids*, Oxford University Press, New York, 1989.
63 D. Frenkel and B. Smit, *Understanding Molecular Simulation*, Academic Press, London, 2002.
64 S. S. Dukhin and A. E. Yaroshchuck, *Kolloidn. Zh.*, 1982, **44**, 884.
65 B. V. Derjaguin, S. S. Dukhin and A. E. Yaroschuck, *J. Colloid Interface Sci.*, 1987, **115**, 234.
66 M. Colic, G. V. Franks, M. L. Fisher and F. F. Lange, *Langmuir*, 1997, **13**, 3129.
67 S. B. Johnson, G. V. Franks, P. J. Scales and T. W. Healy, *Langmuir*, 1999, **15**, 2844.
68 M. Manciu and E. Ruckenstain, *Adv. Colloid Interface Sci.*, 2003, **105**, 63.
69 R. Rahnemaie, T. Hiemstra and W. H. van Riemsdijk, *J. Colloid Interface Sci.*, 2006, **293**, 312.
70 T. Hiemstra and W. H. Van Riemsdijk, *J. Colloid Interface Sci.*, 2006, **301**, 1.
71 D. Gillespie, M. Valiskó and D. Boda, *J. Phys.: Condens. Matter*, 2005, **17**, 6609.

72 K. Wang, Y.-X. Yu, G.-H. Gao and G.-S. Luo, *J. Chem. Phys.*, 2007, **126**, 135102.
73 Z.-Y. Wang and Y.-Q. Ma, *J. Chem. Phys.*, 2009, **131**, 244715.
74 A. Travesset and S. Vangaveti, *J. Chem. Phys.*, 2009, **131**, 185102.
75 A. Martín-Molina, M. Quesada-Pérez, F. Galisteo-Gónzalez and R. Hidalgo-Álvarez, *J. Phys. Chem. B*, 2002, **106**, 6881.
76 A. Martín-Molina, M. Quesada-Pérez, F. Galisteo-Gónzalez and R. Hidalgo-Álvarez, *J. Chem. Phys.*, 2003, **118**, 4183.
77 C. D. Lorenz and A. Travesset, *Phys. Rev. E: Stat., Nonlinear, Soft Matter Phys.*, 2007, **75**, 061202.
78 A. A. Chialvo and J. M. Simonson, *J. Phys. Chem. C*, 2008, **112**, 19521.
79 C. D. Lorenz, P. S. Crozier, J. A. Anderson and A. Travesset, *J. Phys. Chem. C*, 2008, **112**, 10222.
80 C. A. Miller, S. H. Gellman, N. L. Abbott and J. J. de Pablo, *Biophys. J.*, 2008, **95**, 3123.
81 C. A. Miller, S. H. Gellman, N. L. Abbott and J. J. de Pablo, *Biophys. J.*, 2009, **96**, 4349.
82 D. Horinek, A. Herz, L. Vrbka, F. Sedlmeier, S. I. Mamatkulov and R. R. Netz, *Chem. Phys. Lett.*, 2009, **479**, 173.
83 I. Kalcher, D. Horinek, R. R. Netz and J. Dzubiella, *J. Phys.: Condens. Matter*, 2009, **21**, 424108.
84 R. Messina, *J. Chem. Phys.*, 2002, **117**, 11062.
85 P. Linse, *J. Chem. Phys.*, 2008, **128**, 214505.